

# Exactly solvable mixed-spin Ising-Heisenberg diamond chain with the biquadratic interactions and single-ion anisotropy

Onofre Rojas<sup>1\*</sup>, S. M. de Souza<sup>1</sup>, Vadim Ohanyan<sup>2,3†</sup> and Martiros Khurshudyan<sup>2</sup>

<sup>1</sup>*Departamento de Ciências Exatas, Universidade Federal de Lavras, CP 3037, 37200000, Lavras, MG, Brazil.*

<sup>2</sup>*Yerevan State University, A.Manooqian, 1, Yerevan, 0025 Armenia. and*

<sup>3</sup>*Yerevan Physics Institute, Alikhanian Br.2, Yerevan, 0036, Armenia.*

An exactly solvable variant of mixed spin-(1/2,1) Ising-Heisenberg diamond chain is considered. Vertical spin-1 dimers are taken as quantum ones with Heisenberg bilinear and biquadratic interactions and with single-ion anisotropy, while all interactions between spin-1 and spin-1/2 residing on the intermediate sites are taken in the Ising form. The detailed analysis of the  $T = 0$  ground state phase diagram is presented. The phase diagrams have shown to be rather rich, demonstrating large variety of ground states: saturated one, three ferrimagnetic with magnetization equal to 3/5 and another four ferrimagnetic ground states with magnetization equal to 1/5. There are also two frustrated macroscopically degenerated ground states which could exist at zero magnetic field. Solving the model exactly within classical transfer-matrix formalism we obtain an exact expressions for all thermodynamic function of the system. The thermodynamic properties of the model have been described exactly by exact calculation of partition function within the direct classical transfer-matrix formalism, the entries of transfer matrix, in their turn, contain the information about quantum states of vertical spin-1 XXZ dimer (eigenvalues of local hamiltonian for vertical link).

## I. INTRODUCTION

Lattice models of quantum magnetism continue to be in the focus of attention of theoretical condensed matter physicists. Beside of great practical importance connected with description of magnetic and thermodynamic properties of real magnetic materials, this research area is also attractive from the general statistical mechanics and strongly correlated system theory points of view, especially when one deals with exactly solvable strongly interacting many-body system. The diamond chain is a one-dimensional lattice spin system in which the vertical spin dimers alternate with single spins (See figure 1). This model with  $S = 1/2$  is believed to describe the magnetic lattice of mineral azurite,  $\text{Cu}_3(\text{CO}_3)_2(\text{OH})_2$ , which is famous for its deep blue pigmentation[1–4]. Theoretical research of various aspects of diamond chain physics received much attention during last years[5]-[16]. Diamond chain and especially diamond chain with mixed  $(S, S/2)$  spin are shown to have very rich ground state phase diagrams with Haldane and several spin-cluster states which are tensor product of exact local eigenstates of cluster spins [5, 6]. Many other issues of diamond chain physics have been investigated theoretically during last years including Dzyaloshinsky-Moriya term influence on magnetization processes[7], multiple-spin-exchange effects[8], magnetization plateaus[9, 10], magnetocaloric effect[11], e.t.c. Very recently another one interesting feature of diamond chain, possibility of localized magnon excitations, has been also investigated[12].

Especially important issue is the effect of frustration, which is rather strong in antiferromagnetic diamond chain because of triangular arrangement of the sites. Variants of frustrated recurrent lattices with diamond plaquette have been also studied in Refs. [21] and [22]. However, diamond chain is not integrable in general. Thus, the exact analysis of the dynamic and especially thermodynamic properties of diamond chain is a very complicated issue. Nevertheless, one can consider various exactly solvable variants of spin systems possessing diamond chain topology of interaction bonds with simplified structure of interactions[13]-[16]. The diamond chain with only Ising type of interaction have been exactly solved within classical transfer-matrix technique in Ref. [13] revealing reach  $T = 0$  ground state phase diagram. Yet another exactly solvable diamond chains have been considered in Refs. ([14]-[17]), where vertical spin dimers have been taken as quantum ones with  $XXZ$  interaction while interaction between spins localized on vertical dimer sites and spins from the single sites alternating with them is of Ising type. Mapping the system into a single Ising chain within iteration-decoration transformation[18–20] the authors gave complete description of the ground state properties,  $T = 0$  ground state phase diagram as well as thermodynamic functions for all values of vertical dimer spins magnitude  $S$ . In a very recent paper the diamond chain with  $XX$ -interaction has been considered in the Jordan–Wigner formalism[17].

\* email: ors@dex.ufla.br

† email: ohanyan@yerphi.am

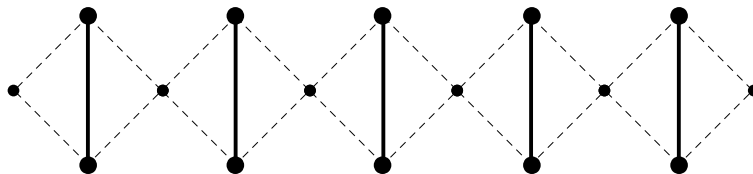


Figure 1: The diamond chain with Ising and Heisenberg bonds. Solid bold lines denote XXZ quantum bonds, dotted lines correspond to Ising interactions. Large(small) circles denote  $\mathbf{S}$  ( $\sigma$ ) spins.

Considering the mixed spin chains (or another one-dimensional spin systems with more complicated geometry) with Ising and Heisenberg bonds (or even just Ising counterparts of the known quantum spin models) one can achieve two-fold goal: to construct novel exactly solvable lattice spin model which allow one to obtain analytic expression for all thermodynamic functions of the model, and to get an approximate models which can be useful for understanding the properties of underlying purely quantum models [14–16, 23–29]. Exact thermodynamic solutions of such models even can shed a light to the properties of real magnetic materials. For instance, for alternating spin chain even simplest models with only Ising interaction can reflect the underlying magnetic behavior of the corresponding Heisenberg counterpart at least in qualitative way [30, 31], moreover, some exactly solvable models with Ising and Heisenberg bonds can also provide satisfactory quantitative picture[29]. Very recently, the synthesis of novel class of trimetallic 3d-4d-4f coordination polymers has been reported. One of them, a 1d coordination polymer compound containing 3d ( $\text{Cu}^{2+}$ ), 4d ( $\text{Mo}^{5+}$ ) and 4f ( $\text{Dy}^{3+}$ ) ions is shown to exhibit the properties of 1d magnet with Ising and Heisenberg bonds[32]. The appearance of Ising interactions between magnetic ion in this compound is connected with the extremely anisotropic properties of  $\text{Dy}^{3+}$  ground states ( $g_{\parallel} = 19.6$ ,  $g_{\perp} \approx 0$ ). Thus, the interactions of  $\text{Dy}^{3+}$  with the surrounding  $\text{Cu}^{2+}$  and  $\text{Mo}^{5+}$  ions are, to the great extent, of Ising type, involving spin projection along the dysprosium anisotropy axis. While, the interaction bonds  $\text{Cu}^{2+}$ — $\text{Mo}^{5+}$  correspond to Heisenberg interaction[32]. Though, the aforementioned 1d coordination polymer system is not exactly the Ising–Heisenberg diamond chain considered in the present paper, this discovery of novel classes of magnetic materials makes the investigation of exact solutions of spin chains with Ising and Heisenberg bonds important from practical point of view as well.

In this paper we consider mixed spin-(1,1/2) diamond chain with Ising and Heisenberg bonds which extends the system considered in Ref. [16] by including biquadratic term for  $S = 1$   $XXZ$ -dimers and single-ion anisotropy. Biquadratic terms are usually originated from the spin-lattice coupling in the adiabatic phonons approximation[33] but also can be considered as the effect of quadrupole interaction between the spins. We do not make any assumption about the origin of biquadratic terms considering them as a part of general Hamiltonian. The model allow one to calculate the partition function and, thus, all thermodynamic quantities exactly within classical transfer-matrix formalism[34]. We present the analysis of  $T = 0$  ground-state phase diagrams and plot the curves of magnetization processes for finite temperatures, demonstrating magnetization plateaus at  $M = 1/5$  and  $M = 3/5$  in the units of saturation magnetization.

The paper is organized as follows. In the second Section we formulate the model and present eigenvalues of block Hamiltonian. In the third section we describe possible ground states of the system and present the ground-states phase diagram. In section 4 we present its exact solution and discuss the magnetization and thermodynamics properties of the model. Finally in sec. 5 a short summary is followed.

## II. THE MODEL AND ITS EXACT SOLUTION

Let us consider the system of vertical  $S = 1$  spin dimers with Heisenberg  $XXZ$  bilinear and biquadratic interactions and uniaxial single-ion anisotropy. These dimers are assembled to the chain by alternating with Ising spins  $\sigma$ , so that each spin  $S$  in certain dimer interacts to its both left and right Ising spins via Ising type interaction (See figure 1). So, we have the so-called diamond-chain with  $S = 1$  Heisenberg dimers and  $\sigma = 1/2$  Ising spins between them. The corresponding Hamiltonian is the sum over the block Hamiltonians:

$$\mathcal{H} = \sum_{i=1}^N \left( \mathcal{H}_i - \frac{\hbar_2}{2} (\sigma_i + \sigma_{i+1}) \right), \quad (1)$$

$$\mathcal{H}_i = J(\mathbf{S}_{i1} \cdot \mathbf{S}_{i2})_{\Delta} + K(\mathbf{S}_{i1} \cdot \mathbf{S}_{i2})_{\Delta}^2 + D \left( (S_{i1}^z)^2 + (S_{i2}^z)^2 \right) + J_0(\sigma_i + \sigma_{i+1})(S_{i1}^z + S_{i2}^z) - h_1(S_{i1}^z + S_{i2}^z),$$

where  $N$  is the number of the unit cells (blocks with two spin-1 and one spin-1/2), while  $i$  correspond the particles at  $i$ -cell.  $J$  being the coupling constant of bilinear  $XXZ$ -interaction between Heisenberg spins, which we assume to be of the following form

$$(\mathbf{S}_{i1} \cdot \mathbf{S}_{i2})_{\Delta} = \Delta(S_{i1}^x S_{i2}^x + S_{i1}^y S_{i2}^y) + S_{i1}^z S_{i2}^z, \quad (2)$$

whereas  $K$  denotes the biquadratic  $XXZ$ -interaction term,  $D$  means the single ion-anisotropy and  $J_0$  being the purely Ising interaction term.  $h_2$  and  $h_1$  are the external magnetic field acting on  $\sigma_i$  and  $S_i$  respectively.

In order to solve this model, at first, we need to diagonalize the block Hamiltonian for arbitrary  $i$ -th block. Nine eigenvalues of  $\mathcal{H}_i$ ,  $\lambda_n(\sigma_i, \sigma_{i+1})$ ,  $n = 1 \dots 9$  can be found analytically, which write down as

$$\begin{aligned} \lambda_{1,2} &= J + K + 2D \pm 2[-h_1 + J_0(\sigma_i + \sigma_{i+1})], \\ \lambda_{3,4} &= \Delta(J + \Delta K) + D \pm [-h_1 + J_0(\sigma_i + \sigma_{i+1})], \\ \lambda_{5,6} &= -\Delta(J - \Delta K) + D \pm [-h_1 + J_0(\sigma_i + \sigma_{i+1})], \\ \lambda_7 &= -J + K + 2D, \\ \lambda_{8,9} &= \frac{-J + (1 + 4\Delta^2)K + 2D}{2} \pm \frac{1}{2}R, \end{aligned} \quad (3)$$

where for simplicity  $R$  denotes the following expression,,

$$R = \sqrt{8\Delta^2(J - K)^2 + (J - K - 2D)^2}. \quad (4)$$

The eigenvectors of block Hamiltonian  $\mathcal{H}_i$  up to the inversion of all spins are

$$\begin{aligned} |v_2\rangle &= |1, 1\rangle, & \Rightarrow & \lambda_1, \lambda_2 \\ |v_{1,s}\rangle &= \frac{1}{\sqrt{2}}(|1, 0\rangle + |0, 1\rangle), & \Rightarrow & \lambda_3, \lambda_4 \\ |v_{1,a}\rangle &= \frac{1}{\sqrt{2}}(-|1, 0\rangle + |0, 1\rangle), & \Rightarrow & \lambda_5, \lambda_6 \\ |v_{0,a}\rangle &= \frac{1}{\sqrt{2}}(-|-1, 1\rangle + |1, -1\rangle), & \Rightarrow & \lambda_7 \\ |v_{0,\pm}\rangle &= \frac{1}{\sqrt{2 + c_{\pm}^2}}(|-1, 1\rangle + c_{\pm}|0, 0\rangle + |1, -1\rangle), & \Rightarrow & \lambda_8, \lambda_9 \end{aligned} \quad (5)$$

where 1, 0 and  $-1$  in first(second) place stand for the  $S^z = 1, 0$  and  $-1$  states for first(second) spin in vertical dimer and the following notation is adopted:

$$c_{\pm} = \frac{1}{2\Delta} \left( 1 + \frac{2D \pm R}{K - J} \right). \quad (6)$$

The eigenvectors of the dimer defined by  $|v_2\rangle$  corresponds to the parallel ordered spins with magnetization per site  $m_s = 1$ , the eigenvectors  $|v_{1,s}\rangle$  and  $|v_{1,a}\rangle$  correspond to symmetric and antisymmetric states vector respectively, whereas  $|v_{0,a}\rangle$  is an antisymmetric state vector with magnetization  $m_s = 0$ , finally  $|v_{0,\pm}\rangle$  are the symmetric eigenvectors with magnetization  $m_s = 0$ .

The remaining eigenvectors of the eigenvalues  $\lambda_2$ ,  $\lambda_4$  and  $\lambda_6$  can be obtaining using the spin inversion.

### A. Special case $K = J$

At the special value  $K = J$  the  $S_{tot}^z = 0$  sector of the block Hamiltonian undergoes qualitative changes which can be obtained substituting carefully  $K = J$  value into the general solution presented above in eq.(5). This should be considered as a consequence of the special symmetry of the Hamiltonian for these values of parameters, more precisely,

the fact that operator  $(\mathbf{S}_1 \cdot \mathbf{S}_2)_\Delta + (\mathbf{S}_1 \cdot \mathbf{S}_2)_\Delta^2$  can be represented in terms of permutation operators  $P_{12}$ . In this case the eigenstates  $|v_{0,a}\rangle$  and  $|v_{0,\pm}\rangle$  of the Hamiltonian reduce to the following ones

$$\begin{aligned} |v_{0,a}\rangle &= \frac{1}{\sqrt{2}}(|1, -1\rangle - |-1, 1\rangle), & \Rightarrow \quad \lambda_7 &= 2D, \\ |v_{0,+}\rangle &= |0, 0\rangle, & \Rightarrow \quad \lambda_8 &= 2J\Delta^2, \\ |v_{0,-}\rangle &= \frac{1}{\sqrt{2}}(|1, -1\rangle + |-1, 1\rangle), & \Rightarrow \quad \lambda_9 &= 2(J\Delta^2 + D). \end{aligned} \quad (7)$$

Note that a straightforward substitution in eq.(6) could yield to an undefined coefficients of the eigenstates.

### III. GROUND STATES PHASE DIAGRAMS

Let us describe possible  $T = 0$  ground states of the chain under consideration and the corresponding energies per block. Generally speaking, there are  $9 \times 2 = 18$  possible ground states for each block. However, if one restricts himself with the ground states which are equivalent up to the inversion of all spins one will arrive at the following spin configurations. The fully polarized state ( $M = 1$ , here  $M$  is magnetization per spin)

$$|SP\rangle = \prod_{i=1}^N |v_2\rangle_i \otimes |\uparrow\rangle_i, \quad \varepsilon_{SP} = J + K + 2D + 2J_0 - \frac{5}{2}H, \quad (8)$$

where  $|\uparrow\rangle_i$  ( $|\downarrow\rangle_i$ ) stands for the up(down) state of the  $\sigma$ -spin in the  $i$ -th block. Hereafter, we also put  $h_1 = h_2 = H$ . The next sector of ground states contains three different ferrimagnetic spin configurations with the value of magnetization equal to  $3/5$  ( $M = 3/5$ ),

$$\begin{aligned} |F1\rangle &= \prod_{i=1}^N |v_2\rangle_i \otimes |\downarrow\rangle_i, \quad \varepsilon_{F1} = J + K + 2D - 2J_0 - \frac{3}{2}H, \\ |F2\rangle &= \prod_{i=1}^N |v_{1,s}\rangle_i \otimes |\uparrow\rangle_i, \quad \varepsilon_{F2} = \Delta(J + \Delta K) + D + J_0 - \frac{3}{2}H, \\ |F3\rangle &= \prod_{i=1}^N |v_{1,a}\rangle_i \otimes |\uparrow\rangle_i, \quad \varepsilon_{F3} = -\Delta(J - \Delta K) + D + J_0 - \frac{3}{2}H. \end{aligned} \quad (9)$$

There are also four another ferrimagnetic ground states with  $M = 1/5$ :

$$\begin{aligned} |F4\rangle &= \prod_{i=1}^N |v_{1,s}\rangle_i \otimes |\downarrow\rangle_i, \quad \varepsilon_{F4} = \Delta(J + \Delta K) + D - J_0 - \frac{1}{2}H, \\ |F5\rangle &= \prod_{i=1}^N |v_{1,a}\rangle_i \otimes |\downarrow\rangle_i, \quad \varepsilon_{F5} = -\Delta(J - \Delta K) + D - J_0 - \frac{1}{2}H, \\ |F6\rangle &= \prod_{i=1}^N |v_{0,a}\rangle_i \otimes |\uparrow\rangle_i, \quad \varepsilon_{F6} = -J + K + 2D - \frac{1}{2}H, \\ |F7\rangle &= \prod_{i=1}^N |v_{0,-}\rangle_i \otimes |\uparrow\rangle_i, \quad \varepsilon_{F7} = \frac{1}{2}(-J + (1 + 4\Delta^2)K + 2D - R) - \frac{1}{2}H. \end{aligned} \quad (10)$$

When no external magnetic field is applied, there are also possibility of frustrated ground state formation, in which the orientation of  $\sigma$  spins in each block are not defined. In this case all  $\sigma$  spins become decoupled and behave like free

spins. There are two frustrated ground states

$$\begin{aligned} |FR1\rangle &= \prod_{i=1}^N |v_{0,-}\rangle_i \otimes |\xi\rangle_i, & \varepsilon_{FR2} &= \frac{1}{2}(-J + (1 + 4\Delta^2)K + 2D - R), \\ |FR2\rangle &= \prod_{i=1}^N |v_{0,a}\rangle_i \otimes |\xi\rangle_i, & \varepsilon_{FR1} &= -J + K + 2D. \end{aligned} \quad (11)$$

Here  $|\xi\rangle_i$  stands for arbitrary value of the  $\sigma$  spin in the  $i$ -th block. Thus, for  $H = 0$  if  $S = 1$  dimer has  $S_{tot}^z = 0$  then its neighboring  $\sigma$ -spins become decoupled which results in macroscopic non-zero entropy  $S/N = \log 2$  for each of the frustrated ground states of Eq. 11. Applying magnetic field one removes the two-fold macroscopic degeneracy driving  $|FR1\rangle$  and  $|FR2\rangle$  ground states into  $|F7\rangle$  and  $|F6\rangle$  respectively. Nevertheless, in some papers two last non-degenerated ground states of eqs.(10) are mentioned as frustrated ones [14–16].

Hereafter, to discuss the phase diagrams we will consider the external magnetic field as  $h_1=h_2=H$ . It is also convenient to present all parameters in the units of  $|J|$ . Thus, we define  $\kappa = K/|J|$ ,  $j_0 = J_0/|J|$ ,  $\delta = D/|J|$  and  $h = H/|J|$ . In Figure 2 one can see four ground states phase diagrams plotted in  $(\kappa, h)$ -plane demonstrating vast variety of ground states for fixed values of the  $\delta$  and  $j_0$ . These plots summarize the effect of biquadratic term. The equations of phase boundaries for  $J > 0, \Delta = 2, j_0 = 0.5$  and  $\delta = 0.5$ (Figure 2(a)) are

$$\begin{aligned} \text{between F7 and SP,} & & h &= \frac{1}{4} \left( 6 - 15\kappa + \sqrt{\kappa^2 + 32(\kappa - 1)^2} \right), & (12) \\ \text{between F7 and F3,} & & h &= \frac{1}{2} \left( -2 - 9\kappa + \sqrt{\kappa^2 + 32(\kappa - 1)^2} \right), \\ \text{between F3 and SP,} & & h &= 4 - 3\kappa. \end{aligned}$$

The rest phase boundaries in this case are either horizontal or vertical lines in  $(\kappa, h)$ -plane.  $F5$  and  $F3$  as well as  $F6$  and  $F1$  are separated by the  $h = 1$  line, while the phase boundary between  $F5$  and  $F6$  as well as between  $F3$  and  $F1$  are vertical line is situated at  $\kappa = 2/3$ . Ground states  $F7$  and  $F5$  are separated by the line  $\kappa = 1/12(-17 + \sqrt{337}) \approx 0.11313$ .

For the case of antiferromagnetic Heisenberg interaction between  $S = 1$  spin ( $J < 0$ ) presented in Figure 2(b) the equations of the phase boundaries are

$$\begin{aligned} \text{between F7 and SP,} & & h &= \frac{1}{4} \left( -15\kappa + \sqrt{32(\kappa + 1)^2 + (\kappa + 2)^2} \right), & (13) \\ \text{between F7 and F2,} & & h &= \frac{1}{2} \left( -4 - 9\kappa + \sqrt{32(\kappa + 1)^2 + (\kappa + 2)^2} \right), \\ \text{between F2 and SP,} & & h &= 2 - 3\kappa, \\ \text{between F4 and F1,} & & h &= 1 - 3\kappa. \end{aligned}$$

The boundary between  $F1$  and saturated ground state  $SP$  is the straight line  $h = 2$ . Horizontal line  $\kappa = 0$  separates  $F4$  and  $F7$  as well as  $F1$  and  $F2$ . In order to demonstrate the significant role of exchange anisotropy  $\Delta$  we plotted also the ground states phase diagrams for the isotropic case  $\Delta = 1$  (Figure 2(c) and (d)) for antiferromagnetic and ferromagnetic  $J$  respectively. One can see simplification of the ground state phase diagram via the disappearance of 2 ground states presented in the case anisotropic case  $\Delta = 2$ (Figure 2(a) and (b)). So, for  $J > 0$  one can find, beside  $SP$ , only  $F3, F5, F7$  and for  $J < 0$  only  $F1$  and  $F7$  ground states respectively. The equation of phase boundaries for antiferromagnetic  $J$ , isotropic  $\Delta = 1$  and  $j_0 = 0.5, \delta = 0.5$  are:

$$\begin{aligned} \text{between F7 and SP,} & & h &= \frac{1}{4} \left( 6 - 3\kappa + \sqrt{8(\kappa - 1)^2 + \kappa^2} \right), & (14) \\ \text{between F7 and F3,} & & h &= \frac{1}{2} \left( -\kappa + \sqrt{8(\kappa - 1)^2 + \kappa^2} \right), \end{aligned}$$

Ground states  $F3$  and  $SP$  are separated by the horizontal line  $h = 3$ , another two straight lines appears between  $F3$  and  $F5$  and  $F7$  and  $F5$  at  $h = 1$  and  $\kappa = 1/7$  respectively. In the case of ferromagnetic  $J$  and isotropic exchange interaction presented in Figure 2(d) one can see only three possible ground states  $F1, F7$  and  $SP$ . Here the horizontal

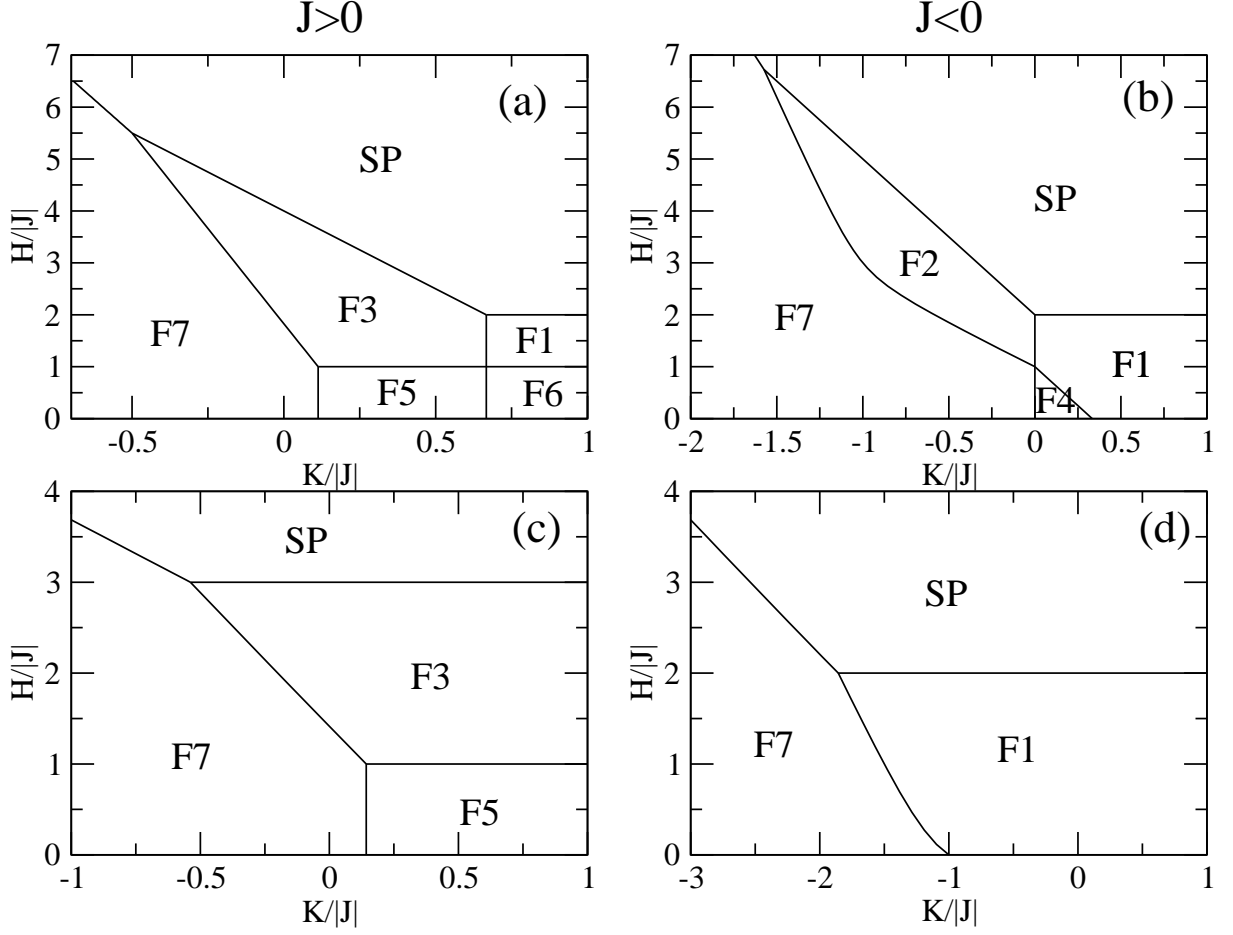


Figure 2: Ground states phase diagrams in  $(\kappa, h)$ -plane demonstrating the effect of biquadratic term. Here  $\kappa = K/|J|$  and  $h = H/|J|$ . The values of all other parameters,  $j_0 = J_0/|J|$ ,  $\delta = D/|J|$  are fixed as follows:  $j_0 = 1/2, \delta = 1/2$ . Left panels ((a) and (c)) corresponds to the antiferromagnetic Heisenberg interaction  $J > 0$ , the right panels ((a) and (c)) - to ferromagnetic one  $J < 0$ . In upper panels ((a) and (b))  $\Delta = 2$  has been taken, while in lower panels ((c) and (d)) one can see phase diagrams for isotropic case  $\Delta = 1$ .

line  $h = 2$  separates  $F1$  and  $SP$  while other two phase boundaries are given by

$$\begin{aligned} \text{between } F7 \text{ and } SP, & \quad h = \frac{1}{4} \left( 6 - 3\kappa + \sqrt{8(\kappa + 1)^2 + \kappa^2} \right), \\ \text{between } F7 \text{ and } F1, & \quad h = \frac{1}{2} \left( 2 - 3\kappa + \sqrt{8(\kappa + 1)^2 + \kappa^2} \right), \end{aligned} \quad (15)$$

In order to summarize the effects of the Ising coupling  $J_0$  we plotted another two ground state phase diagrams presented in Figure 3. Here, the left panel shows ground states boundaries in  $(j_0, h)$ -plane for fixed values of  $\delta, \kappa$  and  $\Delta$ , while right panel demonstrate the phase boundaries for fixed  $\delta, h$  and  $\Delta$  in  $(\kappa, j_0)$ -plane. For the sake of brevity

we just list the equation of phase boundaries. For left panel:

$$\begin{aligned}
\text{between F3 and SP,} & \quad h = \frac{23}{8} + j_0, \\
\text{between F3 and F7,} & \quad h = \frac{1}{2} \left( \frac{\sqrt{11}}{2} - \frac{3}{4} \right) + j_0, \\
\text{between F3 and F5,} & \quad h = 2j_0, \\
\text{between F5 and F1,} & \quad h = \frac{23}{8} - j_0, \\
\text{between F1 and SP,} & \quad h = 4j_0, \\
\text{between F7 and F5,} & \quad j_0 = \frac{1}{2} \left( \frac{\sqrt{11}}{2} - \frac{3}{4} \right), \\
\text{between F3 and F1,} & \quad j_0 = \frac{23}{24},
\end{aligned} \tag{16}$$

For right panel:

$$\begin{aligned}
\text{between F7 and SP,} & \quad j_0 = -\frac{1}{4} \left( 1 + \sqrt{2(\kappa-1)^2 + (\kappa+1)^2} \right), \\
\text{between F7 and F3,} & \quad j_0 = \frac{1}{2} \left( 2 - \frac{3}{2}\kappa - \sqrt{2(\kappa-1)^2 + (\kappa+1)^2} \right), \\
\text{between F7 and F5,} & \quad j_0 = \frac{1}{2} \left( -\frac{3}{2}\kappa + \sqrt{2(\kappa-1)^2 + (\kappa+1)^2} \right), \\
\text{between F7 and F1,} & \quad j_0 = \frac{1}{4} \left( 3 + \sqrt{2(\kappa-1)^2 + (\kappa+1)^2} \right), \\
\text{between SP and F3,} & \quad j_0 = -\frac{3}{2} \left( 1 + \frac{1}{2}\kappa \right), \\
\text{between F3 and F5,} & \quad j_0 = \frac{1}{2}, \\
\text{between F5 and F1,} & \quad j_0 = \frac{3}{2} \left( 1 + \frac{1}{2}\kappa \right).
\end{aligned} \tag{17}$$

Another two ground state phase diagrams demonstrating the influence of single-ion anisotropy are presented in Figure 4. Left(right) panel exhibits phase boundaries for for  $h = 1$ ,  $j_0 = 1$  and  $\Delta = 0.5$  ( $\kappa = 0.5$ ) respectively. The phase boundaries for the left and right panels respectively are

$$\begin{aligned}
\text{between F1 and F7,} & \quad \delta = -\frac{3(2+2\kappa-\kappa^2)}{4(2+\kappa)}, \\
\text{between F1 and F5,} & \quad \delta = \frac{1}{4}(2-\kappa), \\
\text{between F5 and F7,} & \quad \delta = \frac{1}{2} \left( 1 - \kappa + \sqrt{2+10\kappa+1/4\kappa^2} \right),
\end{aligned} \tag{18}$$

and

$$\begin{aligned}
\text{between F1 and F4,} & \quad \delta = \frac{1}{2}(\Delta+1)^2, \\
\text{between F1 and F5,} & \quad \delta = \frac{1}{2}(\Delta-1)^2, \\
\text{between F7 and F4,} & \quad \delta = \frac{1}{2} \left( 1/2 - \sqrt{9/4 + \Delta^4 - 4\Delta^3 + 5\Delta^2 - 6\Delta} \right), \\
\text{between F7 and F5,} & \quad \delta = \frac{1}{2} \left( 1/2 + \sqrt{9/4 + \Delta^4 + 4\Delta^3 + 5\Delta^2 + 6\Delta} \right),
\end{aligned} \tag{19}$$

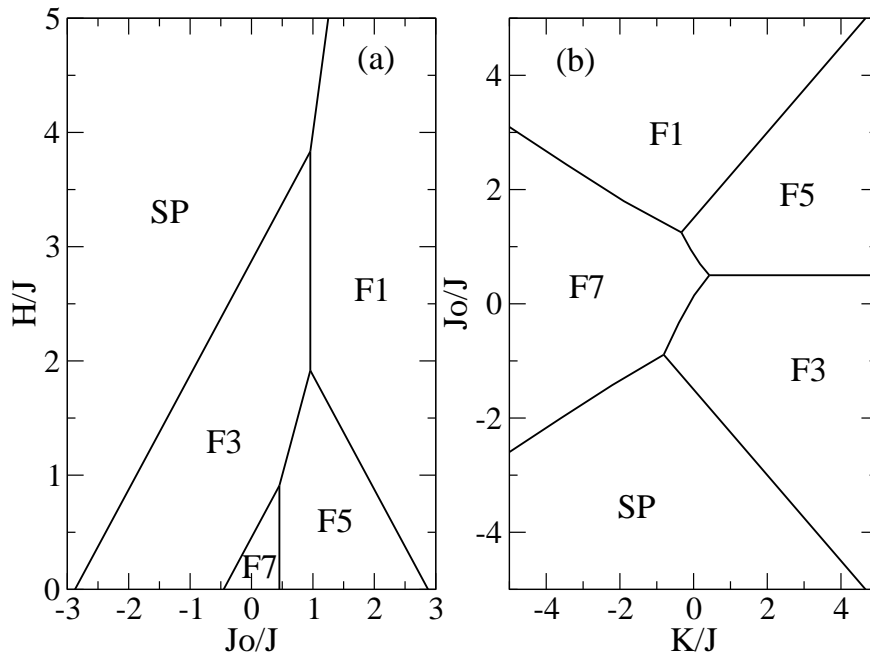


Figure 3: Ground states phase diagrams demonstrating the influence of  $J_0$ . Here  $\Delta = 1/2$ ,  $\kappa = 1/2$  and  $\delta = 1$ . The panel (a) shows the ground states phase diagram in  $(j_0, h)$ -plane for fixed value of biquadratic interaction  $\kappa = 1/2$ ; the panel (b) shows the ground states phase diagram in  $(\kappa, j_0)$ -plane for fixed value of magnetic field  $h = 1$ .

And finally, the zero field ground states phase diagram are presented in Figure 5. The phase diagram exhibits the appearance of two frustrated ground states at zero magnetic field. We choose  $D = 0$  and rather small value of biquadratic interactions  $K = 0.1$ . For convenience we normalize parameters by  $J_0 > 0$ . The equations for the phase boundaries are

$$\text{between F1 and F5,} \quad \tilde{J} = \frac{1 - \tilde{K}(1 - \Delta^2)}{1 + \Delta}, \quad (21)$$

$$\text{between F1 and FR2,} \quad \tilde{J} = 1,$$

$$\text{between FR2 and F5,} \quad \tilde{J} = \frac{1 + \tilde{K}(1 - \Delta^2)}{1 - \Delta},$$

$$\text{between F5 and FR1,} \quad \tilde{J} = \frac{2\Delta - 1 + \Delta(1 + \Delta)(1 + 2\Delta)\tilde{K} + (1 + \Delta(1 + \Delta)\tilde{K})\sqrt{1 + 8\Delta^2}}{2\Delta(1 + \Delta)}, \quad (22)$$

here  $\tilde{J} = J/J_0$  and  $\tilde{K} = K/J_0$ .

#### IV. EXACT SOLUTION AND THERMODYNAMICS

The present model could be solved exactly using the known decoration transformation early presented by M. E. Fisher[18, 19], and recently generalized for arbitrary spin interactions[20], where one maps the partition function of the system to the partition function of 1d Ising model, writing down the relations for the entries of transfer matrix and thus obtaining the relations between model parameters and that of Ising chain. But here we implement a direct

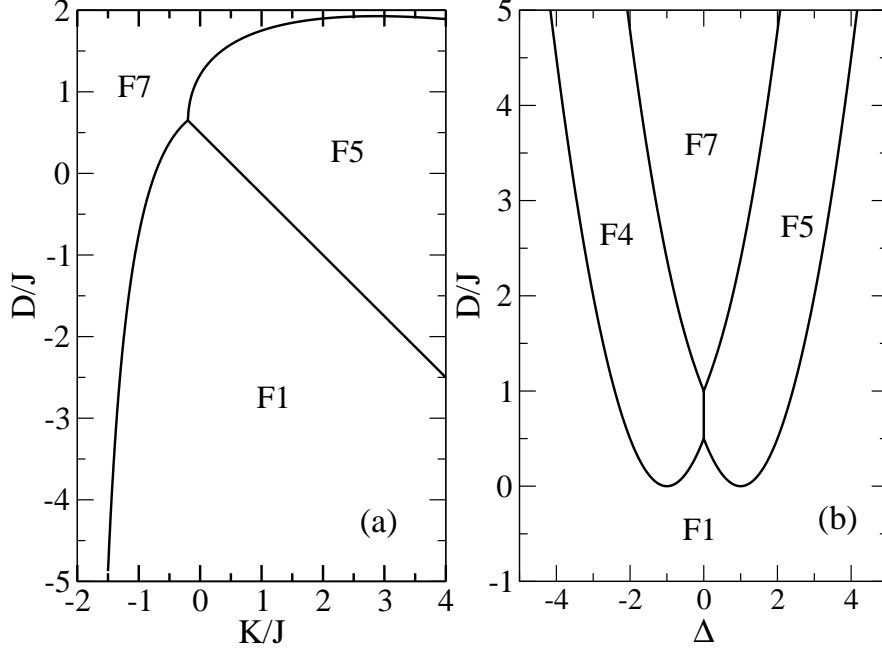


Figure 4: Ground states phase diagrams demonstrating the effect of single-ion anisotropy. Here  $h = 1$ ,  $j_0 = 1$ . Panel (a) exhibit the ground states phase diagram in  $(\kappa, \delta)$ -plane for fixed value of exchange anisotropy  $\Delta = 1/2$ ; panel (b) exhibits the ground states phase diagram in  $(\Delta, \delta)$ -plane for fixed value of biquadratic interaction  $\kappa = 1/2$ .

transfer matrix calculations without any account to the solution of Ising chain. Therefore let us consider the following partition function of the system, which can be represented as

$$\mathcal{Z} = \sum_{\sigma} \text{Sp}_{\mathbf{S}} \exp(-\beta\mathcal{H}) = \sum_{\sigma} \prod_{i=1}^N \exp(\beta \frac{h_2}{2} (\sigma_i + \sigma_{i+1})) Z(\sigma_i, \sigma_{i+1}), \quad (23)$$

where  $\beta$  as usual is inverse temperature. Here

$$Z(\sigma_i, \sigma_{i+1}) = \text{Sp}_i \exp(-\beta\mathcal{H}_i) = \sum_{n=1}^9 \exp(-\beta\lambda_n(\sigma_i, \sigma_{i+1})). \quad (24)$$

Then, using (3) one can express the one-block *partial* partition function  $Z(\sigma_i, \sigma_{i+1})$  in the following form:

$$\begin{aligned} Z(\sigma_i, \sigma_{i+1}) &= \sum_{n=0}^2 Z_n \cosh(\beta n(h_1 - J_0(\sigma_i + \sigma_{i+1}))), \\ Z_0 &= e^{\beta(J-K-2D)} + 2e^{\beta\frac{1}{2}(J-(1+4\Delta^2)K-2D)} \cosh\left(\frac{\beta R}{2}\right), \\ Z_1 &= 4e^{-\beta(\Delta K+D)} \cosh(\beta\Delta J), \\ Z_2 &= 2e^{-\beta(J+K+2D)}. \end{aligned} \quad (25)$$

After that, the partition function (23) take the form similar to the partition function of a chain with classical two

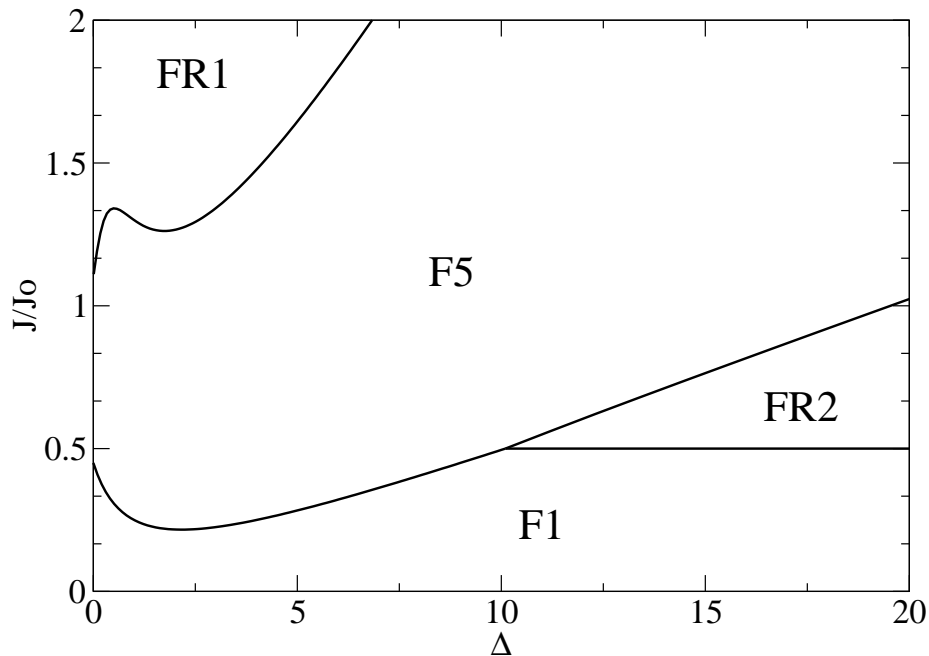


Figure 5: Zero field ground states phase diagram drawn in the  $(\Delta, J/J_0)$ -plane for fixed  $D = 0$  and small values of  $K/J_0 = 0.1$ . The frustrated ground states are exhibited.

state variables on each site:

$$\mathcal{Z} = \sum_{\sigma} \prod_{i=1}^N T(\sigma_i, \sigma_{i+1}) = \text{Sp} \mathbf{T}^N = \Lambda_1^N + \Lambda_2^N, \quad (26)$$

where  $\Lambda_{1,2}$  are two eigenvalues of the transfer-matrix

$$\mathbf{T} = \begin{pmatrix} e^{\beta \frac{h_2}{2}} \mathcal{Z}_+ & \mathcal{Z}_0 \\ \mathcal{Z}_0 & e^{-\beta \frac{h_2}{2}} \mathcal{Z}_- \end{pmatrix}, \quad (27)$$

where

$$\begin{aligned} \mathcal{Z}_{\pm} &= Z(\pm 1/2, \pm 1/2), \\ \mathcal{Z}_0 &= Z(1/2, -1/2) = Z(-1/2, 1/2). \end{aligned} \quad (28)$$

Then, calculating the eigenvalues and taking thermodynamic limit, when only the largest eigenvalue survives, one arrives at the following expression for the free energy per block:

$$f = -\frac{1}{\beta} \log \left( \frac{1}{2} \left( e^{\beta \frac{h_2}{2}} \mathcal{Z}_+ + e^{-\beta \frac{h_2}{2}} \mathcal{Z}_- + \sqrt{(e^{\beta \frac{h_2}{2}} \mathcal{Z}_+ - e^{-\beta \frac{h_2}{2}} \mathcal{Z}_-)^2 + 4\mathcal{Z}_0^2} \right) \right). \quad (29)$$

As soon as the free energy per block is calculated, one can obtain analytic expressions for all thermodynamic function.

### A. Magnetization and quadrupole moment

Magnetic quantities can be obtained using the free energy expression obtained in (29). Therefore the magnetization of the spin- $S$  can be expressed as

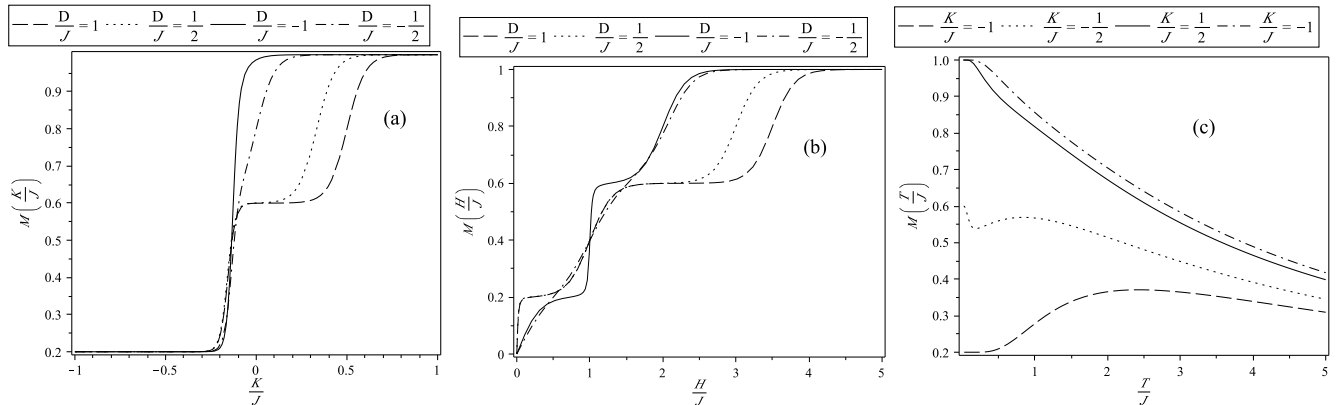


Figure 6: (a) Magnetization as a function of  $K/J$ , for  $H/J = 3.0$ ,  $T/J = 0.15$ ,  $\Delta = 2$  and  $J_0/J = 0.5$ . (b) Magnetization as a function of  $H/J$ , for  $K/J = 0.5$ ,  $T/J = 0.15$ ,  $\Delta = 1$  and  $J_0/J = 0.5$ . (c) Magnetization versus temperature  $T/J$ , for  $J_0/J = 0.5$ ,  $H/J = 4$ ,  $\Delta = 1.4$  and  $D/J = 1$ .

$$M_S = \frac{1}{2N\mathcal{Z}} \sum_{\sigma} \text{Sps} \left( \sum_{i=1}^N (S_{i1}^z + S_{i2}^z) e^{-\beta\mathcal{H}} \right) = -\frac{1}{2} \left( \frac{\partial f}{\partial h_1} \right)_{\beta, h_2, D}, \quad (30)$$

while the magnetization of spin- $\sigma$  reads

$$M_{\sigma} = \frac{1}{N/2\mathcal{Z}} \sum_{\sigma} \text{Sps} \left( \sum_{i=1}^N \sigma_i e^{-\beta\mathcal{H}} \right) = -2 \left( \frac{\partial f}{\partial h_2} \right)_{\beta, h_1, D}. \quad (31)$$

Thus, the total magnetization is given by

$$M = \frac{1}{5} M_{\sigma} + \frac{4}{5} M_S. \quad (32)$$

Figure 6(a) displays the plot of magnetization as a function of biquadratic interaction  $K$  in units of  $J$ , for fixed values of  $H/J = 3$ ,  $T/J = 0.15$ ,  $\Delta = 2$  and  $J_0/J = 0.5$ . Here one can see the plateaus for different values of  $J$ , these plateaus occur as expected at  $1/5$  and  $3/5$ . The plots of magnetization processes ( $M$  versus  $H$ ) for the system under consideration is presented in figure 6(b). Here the values of parameters are fixed as  $K/J = 0.5$ ,  $T/J = 0.15$ ,  $\Delta = 1$  and the value of  $D/J$  varies from  $-1$  to  $1$ . As in can see from the phase diagram in Figure (2)(c), two intermediate magnetization plateaus at  $M = 1/5$  and  $M = 3/5$  exhibited by the system in the case correspond to  $F3$  and  $F5$  ground sates for  $T = 0$ . Thermal behavior of magnetization at the fixed external field is presented in figure 6(c) where the following values of parameters are assumed:  $H/J = 4$ ,  $\Delta = 1.4$ ,  $D/J_0 = 1$  and  $J_0/J = 0.5$ , the competition between ferromagnetic state  $SP$  and ferrimagnetic state  $F1$  with magnetization  $M = 3/5$  is occurred with increase of the temperature. Close to zero temperature one obtains three well defined values for the magnetization, which are in accordance with plateaus displayed in figure 6(a-b).

As the system under consideration contains sites with spin-1 one can define another important physical quantity, quadrupole moment, which can be obtained by the thermodynamic relations as well

$$Q = \frac{1}{2N\mathcal{Z}} \sum_{\sigma} \text{Sps} \left( \sum_{i=1}^N ((S_{i1}^z)^2 + (S_{i2}^z)^2) e^{-\beta\mathcal{H}} \right) = \frac{1}{2} \left( \frac{\partial f}{\partial D} \right)_{\beta, h_1, h_2}. \quad (33)$$

In figure 7(a) the plots of quadrupole moment as a function of  $K/J$  for fixed values of  $H/J = 3$ ,  $J_0/J = 0.5$ ,  $\Delta = 2$  and  $T/J = 0.15$  are presented for several temperatures. The non-trivial and non-monotone behavior of  $Q$  under

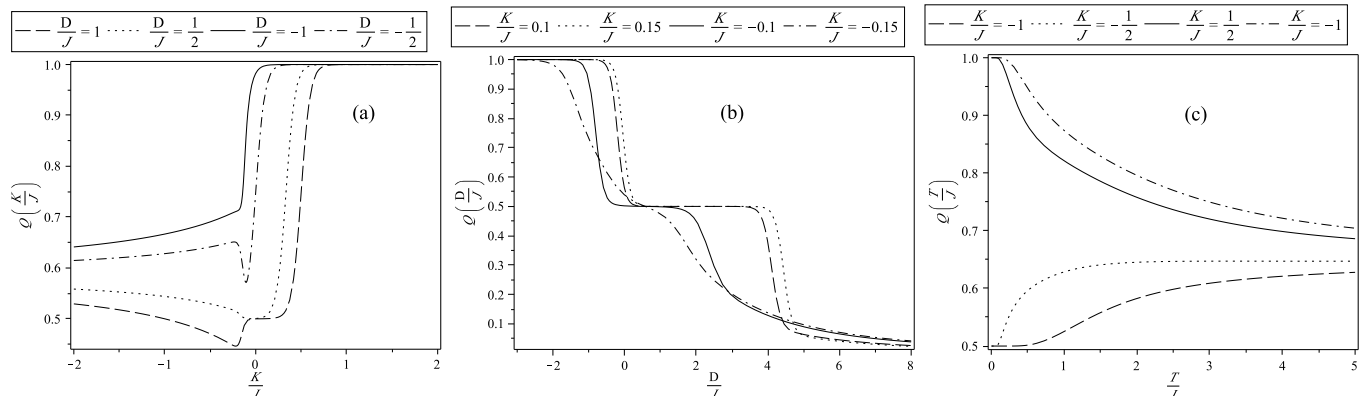


Figure 7: Quadrupole Moment: (a) As a function of  $K/J$ , for  $H/J = 3$ ,  $J_0/J = 0.5$ ,  $\Delta = 2$  and  $T/J = 0.15$ . (b) As a function of  $D$ , for  $J/J_0 = -0.5$ ,  $T/J = 0.1$ ,  $H/J = 2$  and  $\Delta = 2$ . (c) As a function of  $T$ , for  $J_0/J = 0.5$ ,  $D/J = 1.0$ ,  $H/J = 4$  and  $\Delta = 1.4$ .

variation of  $K$  can be understood if one take into account appearance of  $F6$  and  $FR2$  ground states in which vertical quantum dimer is in  $|v_{0,-}\rangle$  eigenstate. Calculating expectation value for the operator  $Q$  for this state one obtains:

$$\langle v_{0,-} | \frac{1}{2} ((S_1^z)^2 + (S_2^z)^2) | v_{0,-} \rangle = \frac{1}{1 + \frac{1}{8\Delta^2} \left(1 + \frac{2D-R}{K-J}\right)^2}, \quad (34)$$

which actually defines low-temperature behavior of the quadrupole moment. The quadrupole moment dependence of the uniaxial single-ion anisotropy parameter  $D$  is illustrated in figure 7(b) for  $H/J = 2$ ,  $J_0/J = -0.5$ ,  $T/J = 0.1$  and  $\Delta = 2$ . Similar to the magnetization case, we obtain some plateaus, but for higher values of  $D$  we have a decreasing curve instead of plateaus (solid line). On the other hand, as soon as the temperature increases these plateaus obviously disappear. In the Figure 7(c) we show the quadrupole moment as a function of the temperature for fixed values of  $J_0/J = 0.5$ ,  $D/J = 1.0$ ,  $H/J = 4$  and  $\Delta = 1.4$ , similar to the case of magnetization (fig.6(c)), the quadrupole moment leads to fixed values at low temperature which are related to the plateaus displayed in figures 7(a-b), while at high temperature average quadrupole moment leads to  $2/3$ , which corresponds to equal probabilities for all three values of  $S = 1$  spin.

## B. Entropy and specific heat

The entropy of the system can be obtained according to general thermodynamic relation,

$$\mathcal{S}(T) = - \left( \frac{\partial f}{\partial T} \right)_{h_1, h_2, D}. \quad (35)$$

One can see the plot of entropy  $\mathcal{S}(T)$  of the model as a function of  $K/J$  in figure 8, here we fix the following values of the parameters:  $J_0/J = 0.5$ ,  $T/J = 0.1$ ,  $\Delta = 3$  and  $D/J = 1$ , assuming the external magnetic field is fixed at  $H/J = 1.0, 0.5$  and  $0.1$ . Three panels correspond to three values of  $\Delta$ , (a)  $\Delta = 0.5$ , (b)  $\Delta = 1$ , (c)  $\Delta = 3$ . A series of peaks corresponding to quantum phase transition points appear on the curve which is in accordance with the phase transition at zero temperature illustrated in figure 2. According to previous discussion, when external magnetic field vanishes there are a residual entropy of the model corresponding to frustrated ground states. This residual entropy is a constant value  $\mathcal{S}(0) = \ln(2) = 0.693$  related to the ground state degeneracy. For particular values of the magnetic field like  $H/J = 1$  it is possible to occur a twofold degeneracy of the ground state energy.

Using the entropy  $\mathcal{S}(T)$ , one can obtain the specific heat

$$C = T \left( \frac{\partial \mathcal{S}}{\partial T} \right)_H. \quad (36)$$

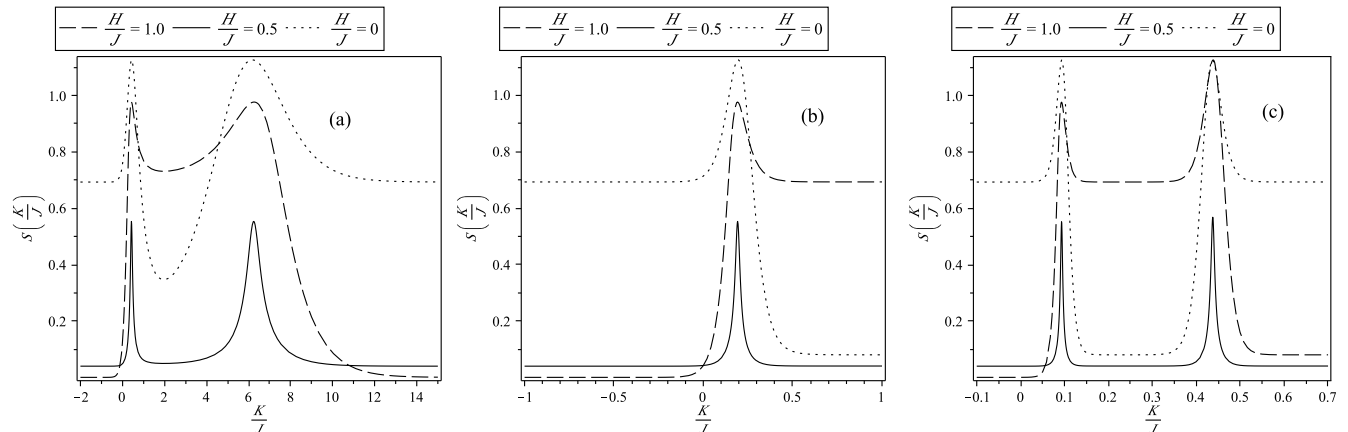


Figure 8: The entropy  $\mathcal{S}(T)$  against  $J$ : assuming fixed values for  $J_0/J = 0.5$ ,  $T/J = 0.1$ ,  $D/J = 1$ . (a)  $\Delta = 0.5$ , (b)  $\Delta = 1$ , (c)  $\Delta = 3$ .

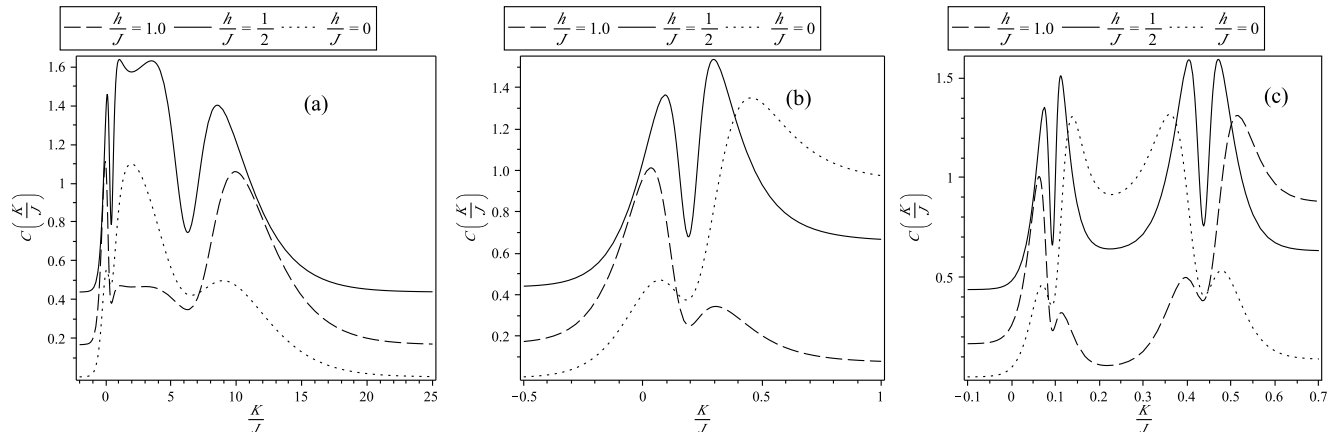


Figure 9: The specific heat  $C(T)$ , for the fixed values of  $J_0/J = 0.5$ ,  $T/J = 0.2$ ,  $J_0/J = -0.5$  and  $D/J = 1$ . (a)  $\Delta = 0.5$ , (b)  $\Delta = 1$ , (c)  $\Delta = 3$ .

In order to study the specific heat properties for the model under consideration, in fig.9 we display the specific heat as a function of the parameter  $K/J$  for the fixed values of  $J_0/J = 0.5$ ,  $T/J = 0.2$  and  $D/J = 1$ . For three values of  $\Delta$ , (a)  $\Delta = 0.5$ , (b)  $\Delta = 1$ , (c)  $\Delta = 3$ . In figure 9 the corresponding plots exhibit four peaks which are related to the phase transition at zero temperature. As one can see the phase transition effects appears for small values of the biquadratic term  $K$ .

## V. CONCLUSIONS

We have considered an exactly solvable variant of diamond chain with mixed  $S = 1$  and  $S = 1/2$  spins. The vertical  $S = 1$  dimers are taken as quantum ones with Heisenberg bilinear and biquadratic interactions and with single-ion anisotropy terms, while all interactions between  $S = 1$  spins and  $S = 1/2$  spins residing on the intermediate sites are taken in the Ising form. The model generalizes the model of diamond chain with Ising and Heisenberg bonds considered in [29]. Our results supplement the previously obtained ones for the case of  $S = 1$  vertical XXZ-dimers with only bilinear Heisenberg interaction. The detailed analysis of the  $T = 0$  ground state phase diagrams is presented as well as the exact plots of various thermodynamic functions. The effect of biquadratic term and single-ion anisotropy are summarized in the corresponding phase diagrams. The phase diagrams have shown to be rather rich, demonstrating large variety of ground states: saturated one, three ferrimagnetic with magnetization equal to  $3/5$  and another four ferrimagnetic ground states with magnetization equal to  $1/5$ . There are also two frustrated

macroscopically degenerated ground states which could exist at zero magnetic field. The thermodynamic properties of the model have been described exactly by exact calculation of partition function within the direct classical transfer-matrix formalism, the entries of transfer matrix, in their turn, contain the information about quantum states of vertical  $S = 1$  XXZ dimer (eigenvalues of local hamiltonian for vertical link). The plots of entropy and specific heat are also presented.

### Acknowledgments

V.O. express his gratitude to Institut für Theoretische Physik Universität Göttingen for warm hospitality during the final stage of this work. This research stay was supported by DFG (Project No. HO 2325/7-1). V.O and M. K. were partly supported by the joint grant of CRDF-NFSAT and State Committee of Science of Republic of Armenia ECSP-09-94-SASP, the work of V. O. was also partly supported by Volkswagen Foundation (grant No. I/84 496) and ANSEF-1981-PS. O.R. and S.M.S thanks CNPq and FAPEMIG for partial financial support.

- 
- [1] F. Aimo, S. Krämer, M. Klajšek, M. Horvatič, C. Berthier, H. Kikuchi, Phys. Rev. Lett. **102**, 127205 (2009).
  - [2] K. C. Rule, A. U. B. Wolter, S. Süllo, D. A. Tennant, A. Brühl, S. Köhler, B. Wolf, M. Lang, J. Schreuer, Phys. Rev. Lett. **100**, 117202 (2008).
  - [3] H. Kikuchi, Y. Fujii, M. Chiba, S. Mitsudo, T. Idehara, T. Tonegawa, K. Okamoto, T. Sakai, T. Kuwai, H. Ohta, Phys. Rev. Lett. **94**, 227201 (2005).
  - [4] B. Gu and G. Su, Phys. Rev. B **75**, 174437 (2007).
  - [5] K. Hida, K. Takano, and H. Suzuki, J. Phys. Soc. Jpn. **78**, 084716 (2009).
  - [6] K. Takano, H. Suzuki, and K. Hida, Phys. Rev. B **80**, 104410 (2009).
  - [7] T. Sakai, K. Okamoto, and T. Tonegawa, J. Phys. : Conf. Series **200**, 022052 (2010).
  - [8] N. B. Ivanov, J. Richter, and J. Schulenburg, Phys. Rev. B **79**, 104412 (2009).
  - [9] H. H. Fu, K. L. Yao, Z. L. Liu, Phys. Rev. B **73**, 104454 (2006).
  - [10] M. S. S. Pereira, F. A. B. F. de Moura, M. L. Lyra, Phys. Rev. B **77** 024402 (2008).
  - [11] M. S. S. Pereira, F. A. B. F. de Moura, M. L. Lyra, Phys. Rev. B **79** 054427 (2009).
  - [12] O. Derzhko, A. Honecker, and J. Richter, Phys. Rev. B **79**, 054403 (2009).
  - [13] J. S. Valverde, O. Rojas, and S. M. de Souza, Physica A **387**, 1947 (2008).
  - [14] L. Čanová, J. Strečka, and M. Jaščur, J. Phys. : Condens. Matter **18**, 4967 (2006).
  - [15] L. Čanová, J. Strečka, T. Lučivjanský, Condens. Matter Phys. **12**, 353 (2009).
  - [16] J. Strečka, L. Čanová, T. Lučivjanský, and M. Jaščur, J. Phys. : Conf. Series **145**, 012058 (2009).
  - [17] T. Verkholyak, J. Strečka, M. Jaščur, and J. Richter *Magnetic properties of the quantum spin-1/2 XX diamond chain: The Jordan-Wigner approach*, arXiv: 1004.0848 (2010).
  - [18] M.E. Fisher; Phys. Rev. **113**, 969 (1958).
  - [19] Syozi, I. *Phase Transitions and Critical Phenomena*, 1, pp. 269-329. Edited by Domb C. and Green M.S., Academic Press, New York, (1972).
  - [20] O. Rojas, J.S. Valverde and S.M. de Souza, Physica A **388**, 1419 (2009).
  - [21] H. Kobayashi, Y. Fukumoto, and A. Oguchi, J. Phys. Soc. Jpn. **78**, 074004 (2009).
  - [22] T. A. Arakelyan, V. R. Ohanyan, L. N. Ananikyan, N. S. Ananikian, M. Roger, Phys. Rev. B **67**, 024424 (2003).
  - [23] J. S. Valverde, O. Rojas, and S. M. de Souza, J. Phys.: Condens. Matter **20**, 345208 (2008).
  - [24] V. Hovhannisyan and N. Ananikian, Phys. Lett. A **372**, 3363 (2008).
  - [25] D. Antonosyan, S. Bellucci, V. Ohanyan, Phys. Rev. B **79**, 014432 (2009).
  - [26] V. Ohanyan, Phys. Atom. Nucl. **73**, 494 (2010).
  - [27] V. Ohanyan, Condens. Matter Phys. **12**, 343, (2009).
  - [28] S. Bellucci and V. Ohanyan, Eur. Phys. J. B **75**, 531 (2010).
  - [29] J. Strečka, M. Jaščur, M. Hagiwara, Y. Narumi, K. Kindo and K. Minami, Phys. Rev. B **72**, 024459 (2005).
  - [30] V. Ohanyan and N. Ananikian, Phys. Lett. A **307**, 76 (2003).
  - [31] F. Litaiff, J. Desousa, and N. Branco, Solid State Commun. **147**, 494 (2008).
  - [32] D. Visinescu, A. M. Madalan, M. Andruh, C. Duhayon, J.-P. Sutter, L. Ungur, W. Van der Heuvel, and L. F. Chibotary, Chem. Eur. J. **15**, 11808 (2009).
  - [33] C. Kittel, Phys. Rev. **120**, 335 (1960).
  - [34] R. Baxter, *Exactly Solved Models in Statistical Mechanics*, (Academic Press, New York, 1982).